S Coda et al.

Non-inductive high-performance discharges on TCV on the path to steady state

Preprint of Paper to be submitted for publication in Special Issue of 30th IAEA Fusion Energy Conference (FEC)



This work has been carried out within the framework of the EUROfusion Consortium, funded by the European Union via the Euratom Research and Training Programme (Grant Agreement No 101052200 — EUROfusion). Views and opinions expressed are however those of the author(s) only and do not necessarily reflect those of the European Union or the European Commission. Neither the European Union nor the European Commission can be held responsible for them.

This document is intended for publication in the open literature. It is made available on the clear understanding that it may not be further circulated and extracts or references may not be published prior to publication of the original when applicable, or without the consent of the Publications Officer, EUROfusion Programme Management Unit, Boltzmannstr. 2, 85748 Garching, Germany or e-mail publications.officer@euro-fusion.org

Enquiries about Copyright and reproduction should be addressed to the Publications Officer, EUROfusion Programme Management Unit, Boltzmannstr. 2, 85748 Garching, Germany or e-mail publications.officer@euro-fusion.org

NON-INDUCTIVE HIGH-PERFORMANCE DISCHARGES ON TCV ON THE PATH TO STEADY STATE

S. CODA¹, C. PIRON², I. VOITSEKHOVITCH⁴, M. AGOSTINI³, F. AURIEMMA³, L. CORDARO³, A. MELE¹, M. PODESTÀ¹, S. GARAVAGLIA⁶, A. JARDIN⁷, M. LA MATINA³, D. MAZON⁶, A. PAU¹, O. SAUTER¹, M. UGOLETTI³, THE TCV TEAM¹⁰, AND THE EUROFUSION TOKAMAK EXPLOITATION TEAM¹¹

*Email: stefano.coda@epfl.ch

Abstract

An extended experimental effort is underway on the TCV tokamak to develop scenarios compatible with long-pulse operation, featuring mostly non-inductively driven current – preferably with a large fraction of bootstrap current. A closely related goal is to achieve good plasma performance, typically measured through the normalized beta β_N . This work is part of a broader endeavor involving several European tokamaks, under the auspices of the Tokamak Exploitation Work Package (WPTE) of EUROfusion, and aimed in part at preparing advanced scenarios for the new JT-60SA tokamak, which is the largest such device ever operated and has these scenarios at the core of its mission. This paper reports on the remarkable progress achieved in the last campaign, featuring an extensive set of discharges sustained over multiple current redistribution times with zero flux contribution from the central solenoid (CS), and approaching stationary conditions with β_N ~2 and ion temperature (Ti) rising to the same order of magnitude as the electron temperature (Te). With increased heating being added in 2026, there is now a realistic prospect of a fully stationary, high- β_N , fully non-inductive NBI-heated scenario. In the process of exploring the boundaries of this scenario, the hot-electron (Te>>Ti) internal-transport-barrier (ITB) regime was also revisited and record temperatures in excess of 12 keV were recorded. Additionally, a fully CS-free current ramp-up, starting only 30 ms after breakdown and displaying robustly negative central magnetic shear, has also been demonstrated. This scenario, which is accompanied by an electron ITB of varying strength, is also a promising step towards a possible spherical-tokamak power plant. Attempts at joining it smoothly to the flat-top advanced-scenario phase have begun.

1. INTRODUCTION

To be commercially viable, controlled nuclear fusion by magnetic confinement is generally believed to have to satisfy a certain number of conditions that are only partially achieved today. High confinement, high performance, low disruptivity, a high degree of stability with minimal-impact residual instabilities, efficient power exhaust, tolerable plasma-wall interactions, long-pulse (ideally steady-state) operation: these are some of the main qualities sought in an eventual power plant. When these are translated to quantitative goals, it is not possible at present to define a single global optimum nor an absolute threshold for each of these properties. It is also not ultimately possible to predict with certainty the extrapolation to reactor size. Research therefore largely proceeds along paths that lead to improvements in one, or preferably more, of these areas, in search of insights and synergies that can thin out the inventory of promising scenarios.

One such path, which is addressed by this paper, focuses on extending the pulse duration [1] while retaining good performance, parametrized primarily by the normalized beta β_N (defined as $\beta_N=aI_p\beta_T/B_T$, where β_T is the ratio of volume-averaged plasma pressure to magnetic pressure, a is the minor radius in meters, I_p is the plasma current in mega-ampere, and B_T is the toroidal magnetic field in tesla). This requires a minimization of the inductive current component, which is the most basic limitation to the pulse length, and preferably a maximization of the bootstrap current fraction. While non-inductive current drive can be provided by high-power electromagnetic waves and neutral-beam injection, the cost and complexity of these external sources is a strong argument for favoring the self-generated plasma bootstrap current, which, in addition, is driven by pressure gradients which go hand-in-hand with high performance. The highest performances in tokamaks have *not* been achieved in highly non-inductive scenarios, and the challenge to improve this state of affairs is motivating an ongoing effort within the Tokamak Exploitation Work Package (WPTE) of EUROfusion on

¹Ecole Polytechnique Fédérale de Lausanne, Swiss Plasma Center (EPFL-SPC), 1015 Lausanne, Switzerland

²ENEA, Fusion and Nuclear Safety Department, C. R. Frascati, Via E. Fermi 45, 00044 Frascati (Roma), Italy

³Consorzio RFX, C.so Stati Uniti 4, 35127 Padova, Italy

⁴CCFE, Culham Science Centre, Abingdon, Oxon, OX14 3DB, United Kingdom

⁵Istituto per la Scienza e la Tecnologia dei Plasmi, CNR, Padova, Italy

⁶ISTP-CNR, via R. Cozzi 53, 20125 Milano, Italy

⁷Institute of Nuclear Physics Polish Academy of Sciences (IFJ PAN), PL-31-342, Krakow, Poland

⁸CRF – University of Padova, Italy

⁹CEA, IRFM, F-13108 Saint Paul Lez Durance, France

¹⁰See author list of B.P. Duval et al 2024 Nucl. Fusion **64** 112023

¹¹See author list of E. Joffrin et al 2024 Nucl. Fusion **64** 112019

multiple devices. A unifying aim is not only to inform ITER operation, where the achievement of long pulses is one of the core objectives albeit at reduced fusion gain Q=5 [2], but more immediately to assist the preparation of long-pulse experiments on JT-60SA [3]. This device, which has recently started operation, is the largest tokamak ever operated, a crucial stepping-stone to reactor conditions, and has these scenarios at the core of its mission. This paper reports on significant progress achieved on the TCV tokamak in the 2024-2025 campaign.

TCV is a conventional-aspect-ratio, mid-sized (R/a=0.88/0.23 m), carbon-walled tokamak (I_p <1 MA, B_T <1.54 T) [4]. It is equipped at present with three electron-cyclotron resonance heating (ECRH) sources, one delivering 0.7 MW in the 2nd harmonic X-mode (X2), and two delivering up to 0.95 MW each in either X2 or X3, through three separate launchers. TCV also features two neutral-beam injectors (NBI), each delivering up to 1.3 MW at 12-28 keV (NBI-1) and 29-52 keV (NBI-2), respectively, and directed tangentially opposite to each other [5]. TCV has an extensive history of steady-state, fully non-inductive discharges with the current driven by X2 electron-cyclotron current drive (ECCD) and bootstrap current [6]. A subset of these shots featured electron internal-transport barriers (eITBs), accompanied by a reverse-magnetic-shear profile with a non-monotonic safety factor [7]. This was a high- β_p scenario (reaching β_p > 2) with bootstrap current fractions routinely larger than 90% – eventually brought to its ultimate limit of fully bootstrap-sustained discharges with no external current drive [8]. This family of discharges relied entirely on electron heating before TCV was equipped with ion heating in the form of NBI, and therefore T_e was invariably much larger than T_i .

The addition of NBI to TCV has opened up a sizable research avenue involving directly reactor-relevant Hmode scenarios with comparable ion and electron temperatures. These NBI-heated scenarios run the gamut from literal ITER-baseline scenarios to more exploratory ones and are the higher-performance extension of a sprawling earlier research line on Ohmic H-modes [9]. Merging T_e~T_i with non-inductive conditions has been seen as a quest to merge the two scenarios described above, which has accordingly been alternately pursued by starting from one or the other, with the expectation of a unified eventual asymptote [10]. The examination of earlier partial successes has resulted in an increased emphasis on the non-inductive element. Key to the work on TCV, and the nature of its unique challenge, is the pursuit of true steady state, made possible – for a nonsuperconducting tokamak – by its modest size (the discharge duration is longer than the current redistribution time) and its very high EC power to volume ratio, which enables non-inductive operation with reasonable current levels. Tailoring the ramp-up phase of the discharge has been seen empirically on TCV to have little effect on the ultimate asymptote, which marks a significant difference from much of the published work on high-beta, long-pulse scenarios [11-17] - which are also primarily ion-heated regimes that are ultimately not directly applicable to a fusion reactor. The TCV path is more closely related to the non-inductive, long-pulse scenarios of the superconducting tokamak EAST [18], which feature substantial electron heating and face a comparable challenge in reaching the highest performance.

Prior to the last campaign, a semi-stationary, non-inductive scenario with good ECRH and NBI coupling – with near-simultaneous power ramps – was obtained, with β_N =1.8 and a 35% bootstrap current fraction, involving internal and external particle transport barriers and a more modest internal temperature barrier [10]. The reproducibility was unsatisfactory, however. While some discharges transited into H-mode and transiently reached β_N up to 2.4, the scenario was plagued by high disruptivity from MHD activity, resulting often from small variations in the density profile.

In the 2024-2025 campaign we set out to build from previous experience and attempt to find a stabler operation space, with guidance from interpretative and predictive transport modeling, primarily with the ASTRA [19] and TRANSP [20] codes. At the same time, we also sought to expand the operating range, by developing a non-inductive current ramp-up as well as by exploring different magnetic topologies for better core-edge integration. Virtually all the discharge phases described in this paper are without a flux contribution from the central solenoid (CS).

The remainder of this paper is structured as follows. Section 2 describes an extension of the eITB operating range during the exploration of the accessible parameter space, resulting in record electron temperatures. The approach to $T_e \sim T_i$ in fully non-inductive conditions and the current best performance are discussed in section 3. Section 4 discusses an alternative topology that has been developed in preparation for first attempts at detachment. The development of fully CS-free current ramp-up scenarios is the subject of section 5. Finally, conclusions and an outlook are offered in section 6.

2. EXTENSION OF THE NON-INDUCTIVE EITB SPACE

Earlier attempts at NBI-heated non-inductive discharges had highlighted a peculiar difficulty inherently caused by the TCV constitutive parameters, namely, that a narrow range is available to advanced tokamak scenarios – in particular in density (if too high, as often caused by NBI fueling, ECRH-X2 is cut off – its cutoff density is 4.3×10^{19} m⁻³; if too low, both NBI coupling and equipartition are weakened, driving T_e well above T_i). A

significant component of this experimental endeavor was then achieving good density control, as well as adjusting the timing of the different heating sources – a related task, as this also strongly affects density. Variable wall recycling, depending on machine conditions, and the pump-out effect induced by core ECRH further complicate density control and reproducibility.

In most of the discharges that were performed in our search for a stable path to high performance, the CS was clamped to a constant current soon after the beginning of the flat top and after the electron-cyclotron heating sources destined to drive most of the current were applied. Any remaining loop voltage would then be small, supplied by whatever non-stationarity remains, i.e., from the time variation of the plasma current and of the currents in the poloidal-field coils involved in the vertical and radial real-time control.

One line of inquiry sought to establish the non-inductive conditions early on, with reverse central shear, and adding NBI later. This exploration had the effect of expanding our well-known eITB scenario. In some cases a more extended core area of increased confinement was seen, rather than a localized barrier, and a record electron temperature of 12 keV (Fig. 1) was attained in a non-inductive shot with one gyrotron used for heating slightly more centrally with a small counter-ECCD component, which has the effect of steepening the reverse magnetic shear and generally results in higher confinement (comparable temperatures were only achieved in the past in inductive discharges, in the so-called ICEC regime [21]). This heating strategy however failed to achieve good performance once ion heating was introduced. With NBI, a progressive degradation of confinement and performance is observed over time, reducing β_N to \sim 1 and failing to lift the ion temperature and maintain the transport barrier at the same time. Through these attempts, we empirically established that good performance and good non-inductive current sustainment require the three existing ECRH beams to be employed for off-axis co-ECCD. Repurposing one beam to heat the center invariably causes an excessive loss in driven current, negating the advantage provided by injecting heat in the highest-confinement region.

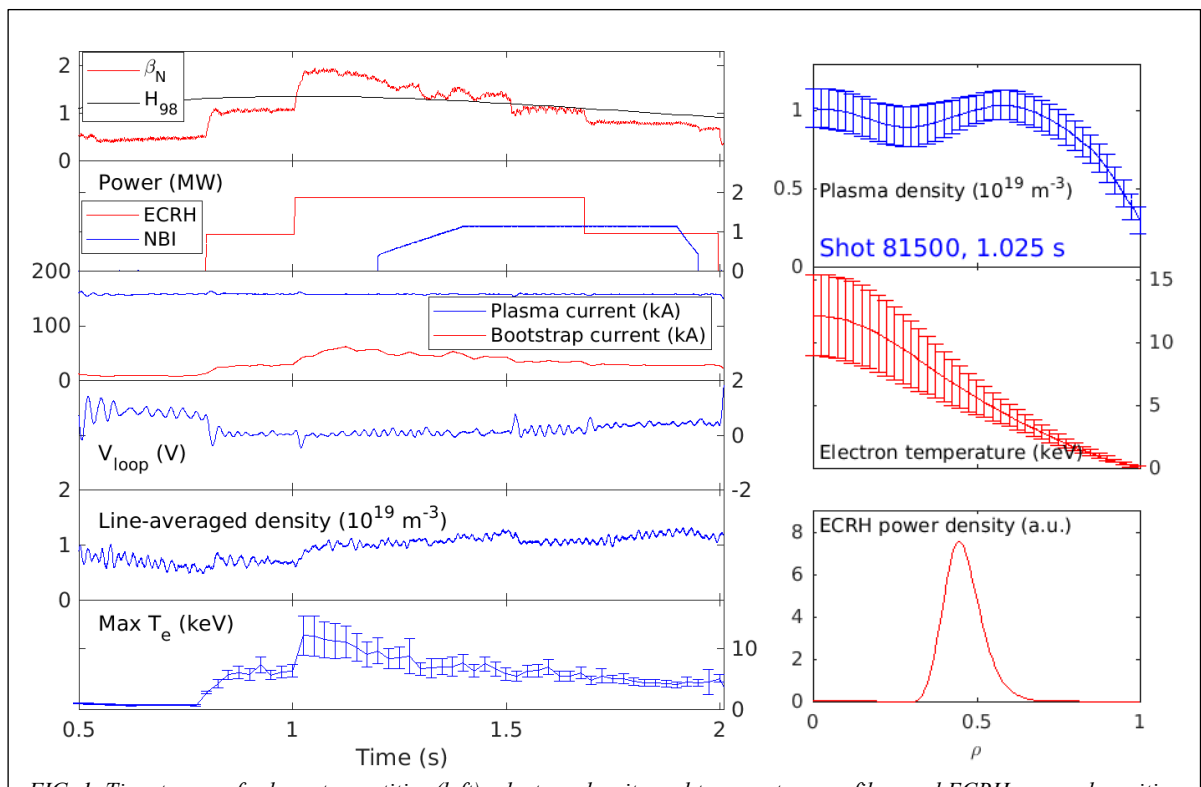


FIG. 1. Time traces of relevant quantities (left); electron density and temperature profiles, and ECRH power deposition profile (calculated by the ray-tracing code TORAY-GA [22]), at the time of maximum β_N (right) for TCV discharge 81500 (with near-zero loop voltage still achieved through plasma current rather than by clamping the CS). The radial variable ρ is the normalized square root of the poloidal flux.

3. FLAT-TOP NON-INDUCTIVE NBI-HEATED SCENARIOS

A more balanced application of NBI and ECRH (all off-axis ECCD) yielded far more promising results in the cases in which density could be controlled within the narrow useful range. Empirically, it was found that, all other factors being equal, beam 2 (NBI-2) at 50-60 keV, injected in the counter-current direction, was better than co-current NBI-1 (20-25 keV) in sustaining high β_N with less virulent MHD activity. This result is not readily understood and is a current object of theoretical investigation. In practice, best results were obtained by injecting both NBI-1 and NBI-2, with an asymptotic, semi-stationary β_N =2 reached during a density rise driven by beam fueling, accompanied by a slow plasma-current descent from an initially stable level of 180 kA (Fig. 2). NBI is injected on the midplane whereas the plasmas used in this study are shifted upwards (Fig. 3, left) to facilitate ECRH launching, so that NBI is deposited off-axis as well. Both TRANSP and ASTRA simulations indicate that the safety-factor shear is reversed in the core (Fig. 2). Neither the density nor the temperature profile features a strong barrier, although local increases in gradient are observed both at mid-radius and near the plasma boundary, and the separatrix density is remarkably high (2x10¹⁹ m⁻³). Consequently, the bootstrap

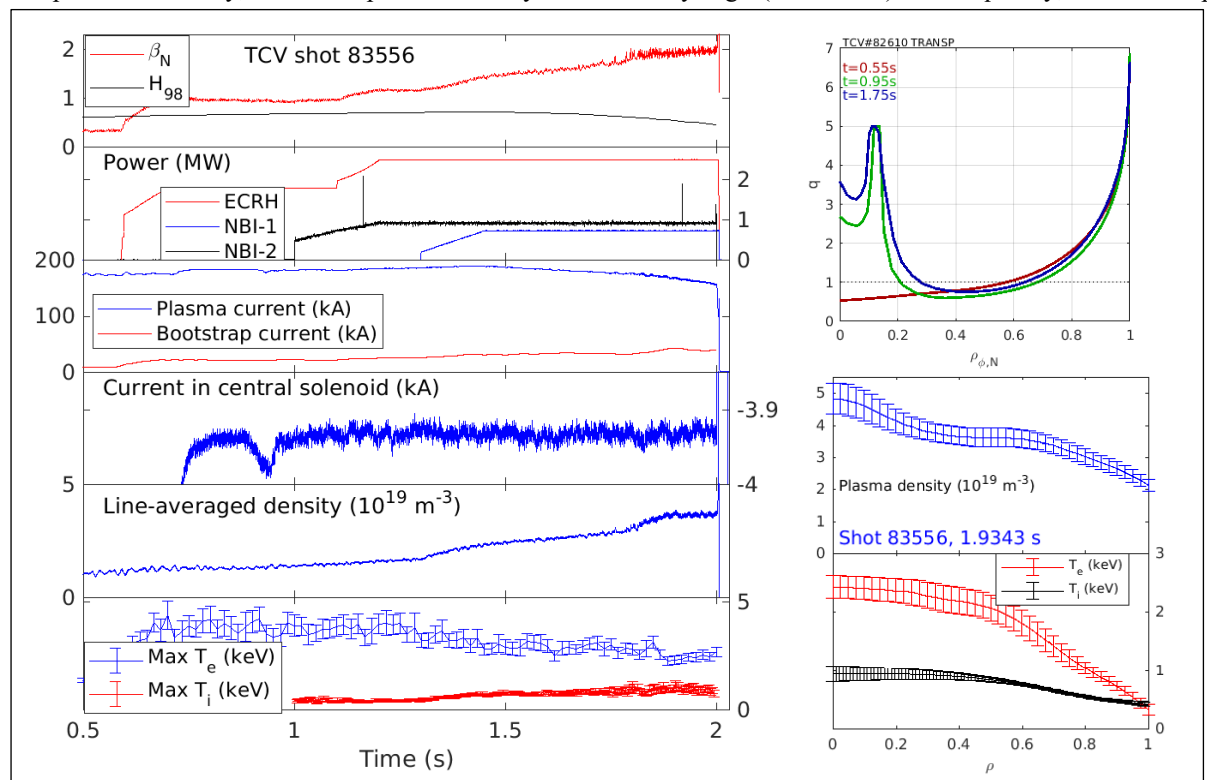


FIG. 2. Time traces of relevant quantities (left) and electron density and temperature profiles near the time of maximum β_N (bottom right) for TCV discharge 83556 with CS current clamped from 0.72 to 2.0 s; safety-factor profile calculated by TRANSP for a shot with very similar time evolution, 82610 (top right).

current fraction remains modest, below 30%. Also, while T_i/T_c rises during the NBI phase, is still does not exceed ~30%.

It is worth mentioning that the more standard lower-single-null diverted configuration used in past experiments had to be abandoned, as the power density on the floor graphite tiles exceeded their power handling capabilities on the leading edges around ports and resulted in several cracks and fractured tiles near the outer strike point. Theoretical tolerances had been exceeded significantly before, but these damages provided for the first time a valuable, real empirical limit. As the inner wall tiles are designed for much higher power handling, these advanced scenarios are now run with both strike points on the inner wall (Fig. 3a).

Magnetic analysis of the MHD modes observed in these discharges reveals mode numbers (m,n) = (2,1), (3,2), and (3,1). Unsurprisingly, their intensity increases with applied power. It is notable that in some analyzed discharges two (3,1) modes at different frequencies are observed both on magnetic and soft-X-ray signals, the latter indicating that they are located at different radial locations. This corroborates the reversal of the q shear in the core predicted by modeling. Empirically, the disruptivity induced by MHD activity appears to correlate with the power deposition location of the off-axis co-ECCD sources – practical recipes were developed for the optimal locations, and the useful range appears to be quite narrow.

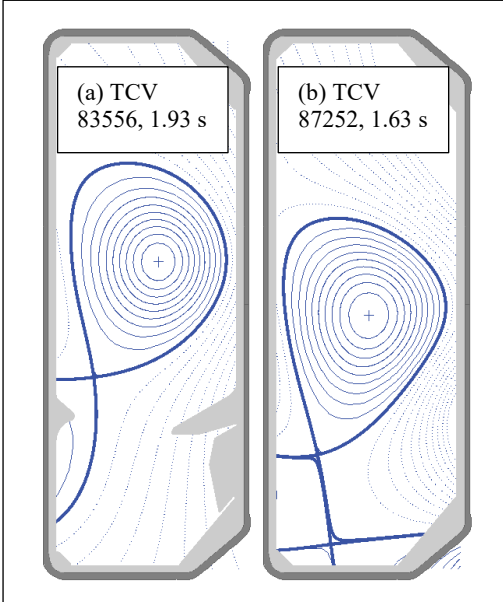
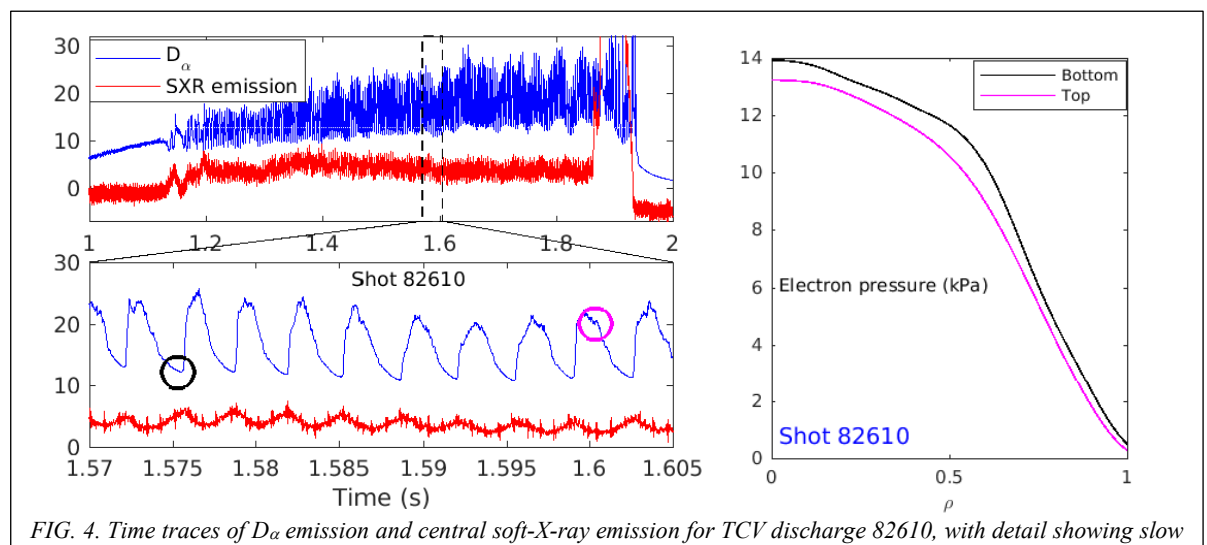


FIG. 3. Flux-surface contours for (a) a standard semi-stationary long-pulse discharge and (b) an X-point target radiator discharge.

From the base scenario with zero flux swing from the CS, a small scan of the induced loop voltage, between -30 mV and +30 mV, was performed, by applying positive or negative slopes to the CS current trace. Positive (co-current) voltage lowers the central safety factor whereas the opposite happens with negative voltage. Within this range, however, the variation in performance (β_N) was negligible. MHD activity was nevertheless mitigated with positive loop voltage. This could arguably lead to a more stable, high-performance scenario at the expense of a modest CS flux contribution, and remains to be studied further, especially in conjunction with increased ECRH power in the future.

A separate phenomenon that is observed in a sizable fraction of the semi-stationary discharges is a slower oscillation of typically 350 Hz visible on many signals, including the D_{α} emission (Fig. 4). This could be described as a periodic relaxation in that it is accompanied by periodic steepening and flattening of the temperature and density pedestal, albeit not as dramatically as in the case of ELMs. Analysis of magnetic probe signals and tomographically inverted soft-X-ray signals suggests that this oscillation is spatially axisymmetric (n=0) with poloidal mode number m=1.

A Thermal Helium Beam (THB) diagnostic [23] was



employed in many of these discharges to image coherent and turbulent fluctuations on the outer midplane at the very edge of the confined plasma and into the scrape-off layer (SOL). Several of the coherent modes detected by magnetics, and presumably associated with rational q surfaces, are also seen by the THB system, and the coherency between the two sets of signals is correspondingly high. The THB signal analysis permits determining that these modes comprise electron-density and electron-temperature oscillations of comparable relative size, which, intriguingly, extend well into the SOL, suggesting that the instabilities cause robust radial transport across the separatrix. A preliminary investigation of the broadband edge turbulence profiles with THB suggests that the turbulence amplitude and statistical properties exhibit no obvious dependence on ECRH power.

n=0 oscillation (left); variation of the electron pressure profile from the bottom to the top of the D_{α} oscillation (right).

The fact that the available ECRH power is entirely devoted to scenario sustainment through off-axis co-ECCD strongly suggests a great potential in adding a fourth ECRH source to heat the center of the high-confinement region – which could increase β_N significantly without an excessive increase in T_e/T_i . Such a fourth source will become available on TCV in early 2026. The MHD stability of such a scenario, of course, remains to be determined, as does the possibility of producing steeper gradients and a larger bootstrap component. The option of using X3 heating remains mostly unexplored. Modeling is expected to be instrumental in suggesting optimized discharge trajectories.

4. NON-INDUCTIVE X-POINT TARGET RADIATOR CONFIGURATION

Any core scenario that aims to be a candidate for a reactor will eventually have to be integrated with an edge configuration that ensures efficient and safe heat and particle exhaust. It is generally accepted that the edge solution will have to include detachment and a very high radiated power fraction. Detachment is generally associated with high density, which at first sight would make it incompatible with the scenarios discussed in this paper. Nevertheless, we are proposing to study the possibility of detachment, and for this we have chosen the recently developed X-point target radiator (XPTR) configuration [24] as one that may have the greatest chance of success. A secondary radiating X-point on the outer leg and near the strike point, well separated from the primary X-point, characterizes this configuration. This is seen to facilitate detachment and expand the operating space with a more stable radiative cooling region.

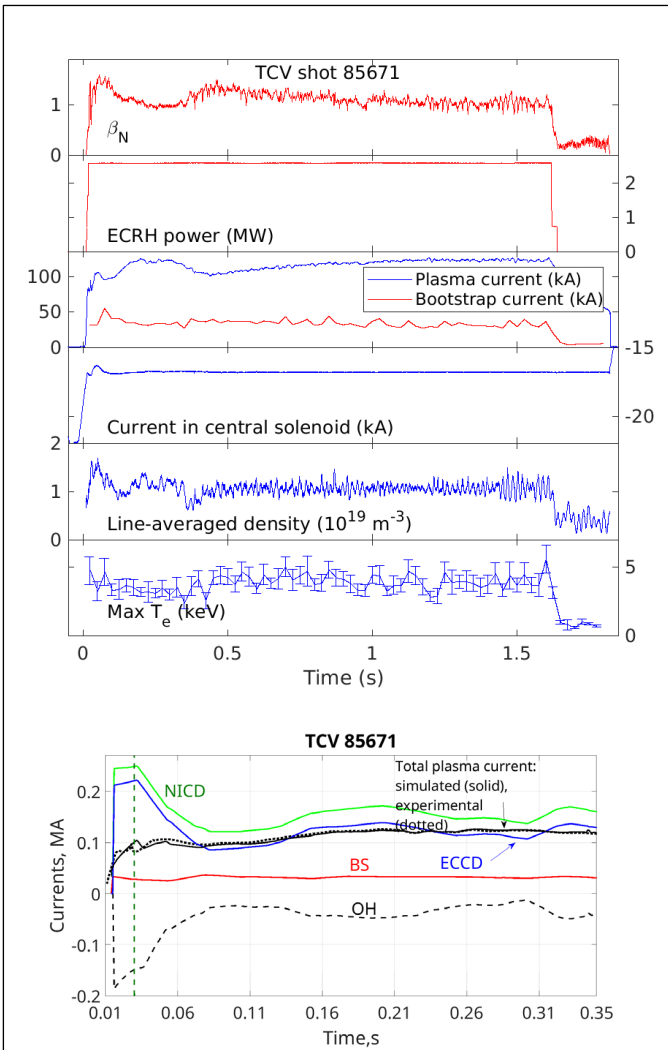


FIG. 5. Time traces of relevant quantities (top), different current contributions simulated with ASTRA using the measured loop voltage as a boundary condition for the current diffusion equation (OH=Ohmic, BS=bootstrap, NICD=non-inductive current drive, ECCD=electron cyclotron current drive) (bottom). The green dashed line indicates the time of clamping the CS to a constant current.

Given the highly exploratory nature of this research avenue, it is felt that the attempt at detachment should be made in a more favorable setup with a partially closed divertor, i.e., with baffles. TCV is periodically equipped with baffles of different lengths so the next such phase will give an opportunity to test this idea. In the last, unbaffled campaign phase we nevertheless set out to develop the scenario in preparation for experiment. An XPTR shape was created (Fig. 3b) by modifying the standard shape described so far in this paper, and CS-free operation was demonstrated with similar ECRH power traces and deposition locations. A recently completed shape controller [25] was employed to optimize the shape and stabilize the secondary X-point beyond what was achievable with pure feedforward programming.

Efficient NBI heating was not achieved so far, with strong MHD activity leading to confinement loss. The ECRH-only phase, however, featured only benign MHD and high electron temperatures > 6 keV.

5. CENTRAL-SOLENOID-FREE DISCHARGE RAMP-UP WITH EITB

One of the devices in which advanced scenarios are being studied within WPTE is MAST-U [26], a spherical tokamak (ST); and one of the primary concerns in view of a possible spherical-tokamak power plant is the elimination of the central solenoid, which would free up space that can in principle allow maximal use of the inherent advantages of the ST approach. In support of this quest, we set out to explore on TCV the possibility of ramping up the plasma current, soon after breakdown, fully non-inductively — or more precisely without using the CS. Ultimately one might also explore a fully CS-free scenario

with EC-assisted breakdown.

For this study, we pursued a similar configuration as in the previous section but applied the EC power 15 ms after breakdown and clamped the CS to a constant current 30 ms after breakdown. Thus, the plasma must evolve without CS assistance through its inner-wall-limited phase, the progressive establishment of shape (elongation, triangularity) and growth in size, through the formation of the divertor and the attainment of the current flat-top phase from 0.43 s. A certain effort was required to keep the desired shape and avoid virulent MHD instabilities particularly during divertor formation; the plasma control system had to be fine-tuned to match the parameters

freely achieved by the plasma – with the CS current clamped, the plasma current cannot be controlled independently and is thus floating freely. With these improvements, a full non-inductive ramp-up was successfully achieved (Fig. 5) with good reproducibility. The CS current is ramped from -22 to -17 kA for breakdown, then clamped – using only approximately 10% of the total flux available.

The operational domain was explored through scans in density, power, and power deposition locations. The reverse-shear q profile is confirmed by interpretative ASTRA [19] simulations: it is formed at the start and lasts throughout the discharge; the value of q_{min} varies considerably within the scans performed. Strong ECCD overdrive is in fact observed, the Ohmic contribution resulting from shaping coils and from the plasma self-inductance being directed counter-current in the ramp-up phase. While a current hole is calculated to occur in some cases, the plasmas do not suffer from double tearing modes.

A steep electron temperature gradient is clearly observed to develop in the core during the ramp, self-consistently with the formation of the reversed shear profile (Fig. 6, top middle and right panels). Following the approach developed in [27] for ITB identification, these ramp-up scenarios are simulated with the L-mode Bohm-gyroBohm (BgB) transport model [28] used with and without the magnetic shear stabilisation multiplier F(s_m) included in the Bohm-like term and validated previously in the reverse/optimized shear configurations on TFTR, DIII-D, and JET. These time-dependent simulations performed with ASTRA for the whole TCV ramp-up phase include the equations for T_e and T_i, solved with the measured density profiles and the q profile obtained from the interpretative current diffusion simulations. The T_e profile predicted with the BgB model matches the

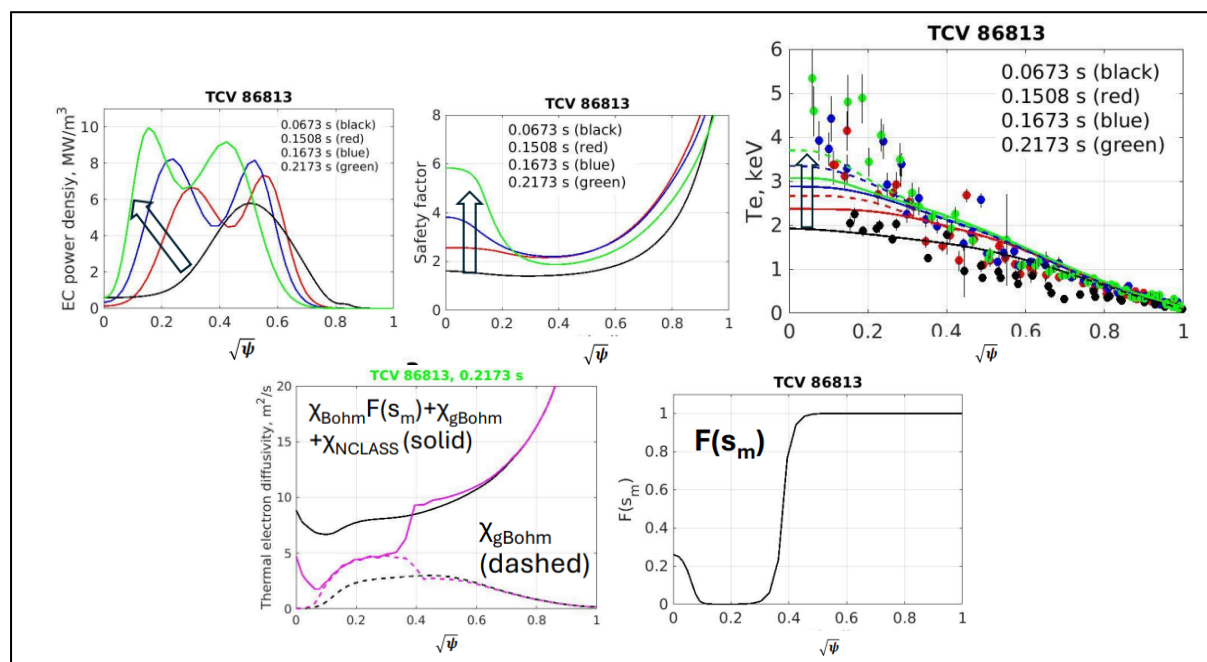


FIG. 6. Evolution of the EC power deposition profile (top left), q profile (top middle) and electron temperature (top right) during the non-inductive current ramp-up phase. Solid and dashed curves in the top right panel show the T_e simulated with the original BgB model [28] and the BgB model containing the magnetic shear stabilisation function $F(s_m)$ [27], respectively. Thermal electron diffusivities computed with (magenta) and without (black) the magnetic shear dependence at 0.2173 s are shown on the bottom left figure, along with the gyroBohm term. The magnetic shear function is plotted in the bottom right figure.

experimental measurements well in configurations with monotonic and flat q profiles where $F(s_m)\sim 1$, with some deviations in the regions affected by MHD activity (Fig. 6 top right, black curve and symbols); however, the experimental core thermal electron confinement in the reverse-shear region is found to be better than the BgB model predictions even in case of fully suppressed Bohm-like transport (Fig. 6 top right, blue and green curves and symbols). The stiffness of the remaining gyroBohm term ($\chi_{gBohm}\sim VT_e$) leading to its increase in the simulations with the $F(s_m)$ term included (Fig. 6, bottom left) may be one of the reasons for the over-estimated thermal diffusivity. It should be mentioned that, in addition to the BgB-based ITB criterion, the existence of a thermal electron ITB in the ramp-up scenario has been confirmed also by using the criterion proposed in [29] and validated in JET ITB plasmas. The thermal ion transport appears to be close to the neoclassical level in this scenario as estimated with ASTRA/NCLASS.

The process of evolving this scenario into the semi-stationary one discussed in section 3 has begun but is unfinished as of this writing.

6. CONCLUSIONS AND OUTLOOK

A key element of long-pulse operation, non-inductive current drive, has been applied to a variety of scenarios on TCV in the pursuit of advanced, high-performance, steady-state regimes. Fully non-inductive, semi-stationary operation has been achieved with strongly improved core confinement leading to record electron temperatures, but also with a combination of electron and ion heating lifting the ion temperature closer to its electron counterpart and a high overall performance with $\beta_N \sim 2$. A non-inductive X-point target radiator has also been demonstrated, in preparation for attempts at detachment. Finally, fully non-inductive ramp-ups are now routinely obtained as well.

This significant progress, however, also confirms that a clear need exists for additional power to make a decisive leap forward. As one additional 1-MW dual-frequency gyrotron is imminent, and a second one is planned for 2027, an exciting new phase beckons.

ACKNOWLEDGEMENTS

This work has been carried out within the framework of the EUROfusion Consortium, partially funded by the European Union via the Euratom Research and Training Programme (Grant Agreement No 101052200 — EUROfusion). The Swiss contribution to this work has been funded by the Swiss State Secretariat for Education, Research and Innovation (SERI). Views and opinions expressed are however those of the author(s) only and do not necessarily reflect those of the European Union, the European Commission or SERI. Neither the European Union nor the European Commission nor SERI can be held responsible for them. This work was supported in part by the Swiss National Science Foundation.

REFERENCES

- [1] LITAUDON, X., et al., Nucl. Fusion 64, 015001 (2024).
- [2] LOARTE, A., et al., Plasma Phys. Control. Fusion 67, 065023 (2025).
- [3] YOSHIDA, M., et al., Plasma Phys. Control. Fusion 64, 054004 (2022).
- [4] HOFMANN, F. et al, Plasma Phys. Control. Fusion 36, B277 (1994).
- [5] DUVAL, B.P., et al., Nucl. Fusion 64, 112023 (2024).
- [6] SAUTER, O., et al., Phys. Rev. Letters 84, 3322 (2000).
- [7] CODA, S., et al., Phys. Plasmas 12, 056124 (2005).
- [8] CODA, S., et al., 22nd IAEA Fusion Energy Conf. (Geneva, Switzerland, 13-18 October 2008), EX/2-3.
- [9] LABIT, B., et al., Plasma Phys. Control. Fusion 66, 025016 (2024).
- [10] CODA, S., et al., 29th IAEA Fusion Energy Conf. (London, UK, 16-21 October 2023), P/3-1939.
- [11] FUJITA, T., et al., Phys. Rev. Letters 87, 085001 (2001).
- [12] POLITZER, P., et al., Nucl. Fusion 45, 417 (2005).
- [13] ISAYAMA, A. and the JT-60 Team, Phys. Plasmas 12, 056117 (2005).
- [14] GAROFALO, A., et al., Nucl. Fusion 55, 123025 (2015).
- [15] HOBIRK, J., et al., Nucl. Fusion 63, 112001 (2023).
- [16] VAN MULDERS, S., et al., Nucl. Fusion 64, 026021 (2024).
- [17] KIM, H.-S., et al., Nucl. Fusion 64, 016033 (2024).
- [18] SONG, Y., et al., Sci. Adv. 9, eabq5273 (2023).
- [19] PEREVERZEV, G.V., et al, Nucl. Fusion 32, 1023 (1992).
- [20] GOLDSTON, R.J., et al., J. Comput. Phys. 43, 61 (1981).
- [21] PIETRZYK, Z.A., et al., Phys. Rev. Letters 86, 1530 (2001).
- [22] MATSUDA, K., IEEE Trans. Plasma Phys. 17, 6 (1989).
- [23] LA MATINA, M., et al., Plasma Phys. Control. Fusion 67, 085034 (2025)
- [24] LEE, K., et al., Phys. Rev. Letters 134, 185102 (2025).
- [25] MELE, A., et al., 10th International Conference on Control, Decision and Information Technologies (CoDIT), Vallette, Malta, 2024, pp. 284-289.
- [26] MORRIS, A.W., IEEE Trans. Plasma Sci. 40, 682 (2012).
- [27] VOITSEKHOVITCH, I., et al., Phys. Plasmas 6, 4229 (1999).
- [28] ERBA, M., et al., Plasma Phys. Control. Fusion 39, 261 (1997).
- [29] TRESSET, G., et al., Nucl. Fusion 42, 520 (2002).